Acta Cryst. (1994). B**50**, 182–191

X-ray Diffraction Study of the Disorder-to-Order Transition at ~160 K in the π-Molecular Compound Pyrene···Pyromellitic Dianhydride

BY FRANK H. HERBSTEIN†

Department of Chemistry, Technion-Israel Institute of Technology, Haifa 32000, *Israel*

AND STEN SAMSON

Noyes Laboratories of Chemical Physics, California Institute of Technology, Pasadena, CA 91125, *USA*

(*Received* 2 *August* 1993; *accepted* 21 *October* 1993)

Abstract

The crystal structure of pyrene···pyromellitic dianhydride [($C_{16}H_{10}$:$C_{10}H_2O_6$); PYRPMA] has been studied over the range 300–19 K, using the low-temperature accessory designed by Samson, Goldish & Dick [*J. Appl. Cryst.* (1980), **13**, 425–432] for a four-circle diffractometer. Earlier results for the disordered and ordered structures [Herbstein & Snyman (1969). *Philos. Trans. R. Soc. London Ser. A*, **264**, 635–666] are confirmed and extended. At 295 K, a = 13.94 (1), b = 9.34 (1), c = 7.31 (1) Å, β = 93.65 (9)°, space group $P2_1/a$, Z = 2, with pyrenes and pyromellitic dianhydrides (PMDAs) at crystallographic centres of symmetry. At 19 K, a = 13.664 (3), b = 9.281 (2), c = 14.420 (3) Å, β = 91.80 (2)°, space group $P2_1/n$, Z = 4, with two sets of pyrenes at independent centres of symmetry and the four PMDAs at general positions. There are no discontinuities in cell dimensions with temperature (measurements at ~10 K intervals, down to 19 K) but db/dT and $d\beta/dT$ show discontinuities at ~167 K. Superlattice reflections appear below ~164 K (= T_c by X-ray diffraction), corresponding to the doubling of c and change of space group; the specific heat shows an anomalous increase over the range 120–155 K, giving a λ-type peak. These results show that the transition is second order with regard to Ehrenfest's criteria. PYRPMA is a co-elastic crystal and quantitative analysis shows a linear dependence of the squares of spontaneous strain and of normalized superlattice intensity on temperature; hence, in terms of Landau theory, the transition is tricritical. However, the excess specific heat cannot be explained entirely on this basis. The physical nature of the transition is discussed. PYRPMA is so far unique among the π-molecular compounds showing disorder-to-order transitions in the solid state in that there is a doubling of one of the axes; all indications are, however, that it resembles the other examples in the sense that subtle intermolecular packing interactions (here between pyrenes and PMDAs) are the driving force for the transition rather than electronic or charge-transfer interactions.

1. Introduction

By far the most common structure type among crystalline π-π* charge-transfer molecular compounds is the mixed-stack arrangement, in which donor and acceptor components alternate along the stack axis (Herbstein, 1971). There is now evidence from various experimental techniques that many such crystals undergo phase transitions on cooling (Parsonage & Staveley, 1978). For example, this has been demonstrated for pyrene···pyromellitic dianhydride (PYRPMA) by X-ray diffraction (Herbstein & Snyman, 1969; HS69) and calorimetric (Dunn, Rahman & Staveley, 1978; Boerio-Goates & Westrum, 1980) methods. The desirability of comparing calorimetric and diffraction results has provided the incentive for extending the earlier (photographic) diffraction measurements by using the more powerful diffractometric instrumentation now available for low-temperature crystal structure analysis (Samson, Goldish & Dick, 1980) and modern computing facilities.

We report in a companion paper (Herbstein, Marsh & Samson, 1994; HMS94) the determination of the crystal and molecular structure of PYRPMA at 19 K, the lowest temperature attainable with the present apparatus. The crystal structure of PYRPMA at 295 K has been redetermined by Allen, Boeyens & Levendis (1989) and described in terms of a model in which the pyrenes are statically disordered over three orientations.

The earlier X-ray studies on PYRPMA showed that there are mixed stacks of alternating pyrene and PMDA molecules in the 295 K structure, both moieties being located at crystallographic centres (space group $P2_1/a$, Z = 2). The c axis was found to have doubled on cooling to ~110 K and the space group changed to $P2_1/n$. There were now two pairs of pyrenes at independent centres, with the four PMDA molecules in the cell at general positions, but only slightly displaced from their 295 K positions. The transition was single

† Experimental work performed while on sabbatical leave at Caltech.

crystal-to-single crystal, with the conservation of axial directions. We note here two corrections to the earlier diffraction study: oscillation photographs (iii) and (iv) in Fig. 2 should be interchanged and it is now clear that the reported temperatures suffered from appreciable systematic errors.

The two sets of calorimetric measurements, which are in good mutual agreement (Fig. 1 and also Fig. 6), showed a small λ-type anomaly at $\sim$155 K, with the enthalpy and entropy of the transition calculated as 222 J mol^{-1} and 1.34 J mol^{-1} K, respectively, by Boerio-Goates & Westrum (1980).

This report is divided into two separate, but related, parts. The first gives results for the order–disorder transition at $\sim$160 K in order to provide more evidence on the nature of the transition, and includes measurement of cell dimensions over the range 19–295 K and of superlattice intensities over the range 19–165 K. The experimental measurements are analysed at two levels, firstly on the basis of Ehrenfest's criteria for determining the order of a transition and then, more quantitatively, in terms of Landau theory, using the temperature dependence of spontaneous strain and superlattice intensities to show that the transition is tricritical. This conclusion is then checked against the excess specific heat, the agreement being incomplete. Our results are compared with those reported for a number of related systems. The second part gives thermodynamic calculations on the molecular compound based on thermodynamic measurements from the literature.

2. Experimental

2.1. *General*

Crystals (bright red in colour, elongated along [001] and showing {100} and {110}) were grown from butan-2-one (dried over $CaCl_2$). After preliminary oscillation and Weissenberg photography (Ni-filtered Cu $K\alpha$), all measurements were made using a modified Syntex $P\bar{1}$ four-circle diffractometer (graphite-monochromated Mo $K\alpha$, $\langle\lambda\rangle$ = 0.71069 Å).

The crystal and measurement systems were stable over the 5-week measurement period. The crystal temperature could be varied between 300 and 19 K and was stable to within 1–2 K. One crystal (approximately a cube of 0.3 mm edge) was used for the measurements of the intensities at 295 K and of the cell dimensions down to 100 K; it then split and was discarded. A second crystal (the same shape as the first but about half its volume) was used for all other measurements. Superlattice intensities reached equilibrium values within *ca* 1 h at each new temperature setting, even at 19 K. We were not able to measure the kinetics of the ordering process because it also takes about 1 h for the cold shell enclosure to reach equilibrium. All measurements were made on crystals at equilibrium. No hysteresis of the intensities or cell dimensions was encountered under our experimental heating and cooling regimens.

Table 1. *Cell dimensions* (Å, °, Å^3) *measured with special care at four temperatures*

The values labelled 295 (ABL) are from Allen, Boeyens & Levendis (1989).

T (K)	a	b	c	β	V
19	13.664 (3)	9.281 (2)	14.420 (3)	91.80 (2)	1827.7 (7)
137	13.701 (6)	9.329 (4)	14.490 (4)	92.45 (3)	1850.4 (13)
160	13.719 (8)	9.352 (5)	14.513 (6)	92.70 (5)	1860.0 (17)
232	13.808 (11)	9.349 (7)	7.293 (4)	93.22 (5)	939.9 (11)
295	13.94 (1)	9.34 (1)	7.31 (1)	93.65 (5)	949.8 (15)
295 (ABL)	13.885 (4)	9.303 (2)	7.307 (4)	93.50 (3)	942.1

2.2. *Cell dimensions*

These were measured at $\sim$10° intervals over the range 19–295 K, in both cooling and heating regimens. Most measurements were made using the auto-centring program of the diffractometer based on nine strong reflections in the region $17 > 2\theta > 25°$. These results were supplemented with more precise measurements (slower scan speed, additional reflections, including some at higher angles) at four widely spaced temperatures (see Table 1). The agreement was satisfactory.

2.3. *Intensities*

Details of measurements are given in HMS94. Quantitative checks showed the same temperature dependence for the intensities of 17 of the stronger superlattice reflections (*i.e.* those with l odd in the ordered structure) and it was inferred that this held for all the superlattice reflections.

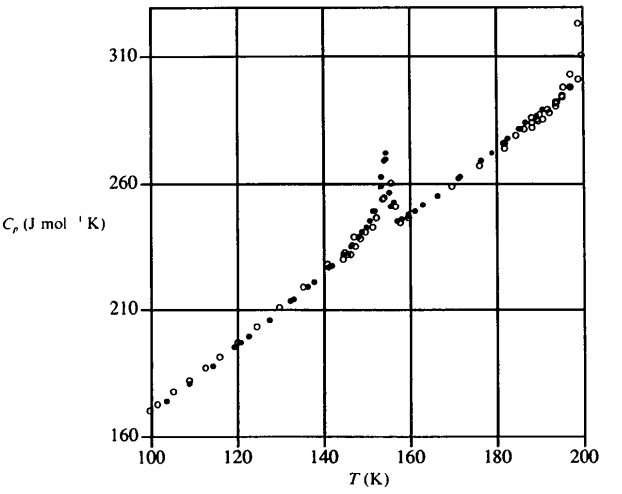

Fig. 1. Specific heat of PYRPMA, according to Dunn, Rahman & Staveley (1978) (open circles) and Boerio-Goates & Westrum (1980) (filled circles). The specific heat is a smooth function of temperature outside the range shown.

3. The order–disorder transition

3.1. *The experimental results*

3.1.1. *Cell dimensions as a function of temperature.* The temperature dependence of the cell parameters is shown in Fig. 2 and Table 1. We have fitted separate quadratic expressions to the cell dimensions in the regions $T \leq T_c$ and $T > T_c$ and these are given in the caption to the figure; T_c is taken as 167 (2) K. Use of such expressions presumably has some theoretical justification in the lower of these temperature ranges but in the higher range it is no more than an exercise in curve fitting.

The most striking feature of the cell-dimension–T curves is the expansion of b on cooling from 300 to ~165 K; this is followed by the more usual contraction on further cooling. The first derivative of the b–T curve has a discontinuity at 165 K – the critical temperature T_c is indicated by this cusp. The β–T curve has a cusp at about the same temperature. The a–T and c–T curves show much less pronounced features around 165 K, which are perhaps better described as changes of slope. As $V = abc\sin\beta$, the V–T curve must also show a cusp at T_c (see also Fig. 4). Our a and b values at 295 K differ significantly from those of Allen, Boeyens & Levendis (1989), although (as pointed out by one of the referees) both sets have a/b = 1.4925; we have not found an explanation. The cell dimensions given in Fig. 2 for the disordered form have been extrapolated ('by eye') into the region of stability of the ordered form for use in the calculation of the spontaneous strain (see §3.3 below).

The b–T and β–T polynomials over the two temperature ranges (see caption to Fig. 2) both intersect at T_c = 167 K, slightly higher than the value of 165 K at which the intensities of the superlattice reflections become zero (see below). The start of the specific heat anomaly (on cooling) is at 158 K and the peak at 155 K (Figs. 1 and 6). Thus, the gross discrepancy (with regard to temperature) between the specific heat measurements and the diffraction measurements of HS69 has now been eliminated, but the present diffraction measurements are not precise enough to establish T_c as 165 or 167 K instead of the specific heat value of 155 K. In the discussions below, we use whichever T_c value best fits the particular data set.

Parameter thermal expansion coefficients {defined here as $[(1/X)(\partial X/\partial T)]$, where $X = a, b, c, \beta$} are shown in Fig. 3. The values extrapolate close to zero at 0 K, as would be expected. Discontinuities at the critical temperature are well established for $[(1/X)(\partial X/\partial T)]$, $X = b, \beta, V$, only the first of which is shown in Fig. 3, but those for $X = a, c$ are less certain as they depend on the curve-fitting process.

The thermal expansion tensors above and below T_c have been determined (Table 2) from the thermally induced changes of the Bragg angles of certain reflections using a *FORTRAN* program (*ALPHA*) written by Jessen & Küppers (1989, 1991), which also diagonalizes the tensor. We have used a number of pairs of temperatures, both below and above T_c, for these calculations; the same qualitative behaviour is found, although there is some dependence on the choice of temperatures. The combinations given below are for reasonably wide

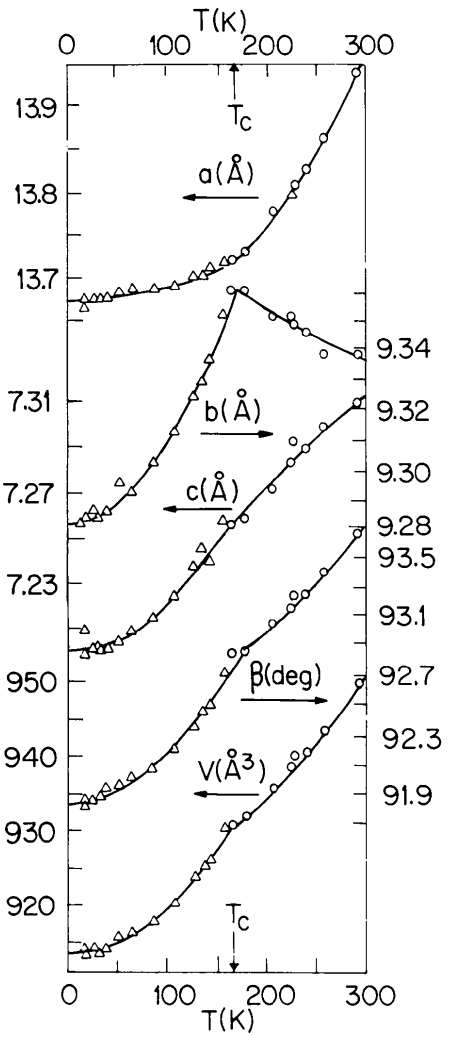

Fig. 2. $a(T)$ plotted against T (K); there is a change of slope in the region of T_c (167 K) but no cusp. Below T_c the points are fitted to a = 13.672 + 1.633 × $10^{-5}T$ + 1.619 × $10^{-6}T^2$, and above T_c to a = 13.701 – 8.258 × $10^{-4}T$ + 5.539 × $10^{-6}T^2$. $b(T)$ plotted against T (K); there is a cusp at T_c (167 K). Below T_c the points are fitted to b = 9.281 + 1.416 × $10^{-5}T$ + 2.558 × $10^{-6}T^2$, and above T_c to b = 9.406 – 3.067 × $10^{-4}T$ + 2.527 × $10^{-7}T^2$. $c(T)$ and $c(T)/2$ plotted against T (K). The ordinate values below T_c (167 K) must be doubled. There are indications of a change of slope at T_c (167 K). Below T_c the points are fitted to c = 14.403 – 1.801 × $10^{-4}T$ + 5.424 × $10^{-6}T^2$, and above T_c to c = 7.165 + 6.128 × $10^{-4}T$ – 3.928 × $10^{-7}T^2$. $\beta(T)$ plotted against T (K). There is a cusp at T_c (167 K). Below T_c the points are fitted to β = 91.806 + 6.808 × $10^{-4}T$ + 2.868 × $10^{-5}T^2$, and above T_c to β = 92.370 + 3.967 × $10^{-4}T$ + 1.340 × $10^{-5}T^2$. $V(T)$ [or $V(T)/2$] plotted against T (K). There is a cusp at T_c (167 K). Below T_c the points are fitted to V = 1826.90 – 2.151 × $10^{-2}T$ + 1.3874 × $10^{-3}T^2$, and above T_c to V = 918.64 + 2.391 × $10^{-2}T$ + 2.745 × $10^{-4}T^2$.

temperature ranges and smooth behaviour of the X–T curves.

Two of the principal components of the symmetrical second-order tensor $[\alpha_{ij}]$ are positive and one is negative, both above and below T_c. Thus, the representation quadric is a hyperboloid of one sheet in both phases (Nye, 1967, p. 18); however, the orientations of these quadrics with respect to the crystal axes are quite different in the two phases. We have shown the representation quadrics diagrammatically in Fig. 4. In the disordered phase the positive coefficient of expansion on cooling is along [010] (see Figs. 6–8 of HMS94), adjacent stacks along this axis thus slightly repelling one another until T_c is reached; as cooling is continued, their relative movement is reversed. In the ordered phase there is an expansion on cooling along [221], which is the direction in which the close pyrene···PMDA approaches (see Fig. 8 of HMS94).

Hyperboloids of one sheet are also found as the representation quadrics of the thermal expansion tensors of (monoclinic) 9-hydroxyphenalone at 145 and 360 K (Svensson & Abrahams, 1986), where there is a reversible first-order disorder-to-order (on cooling) phase transformation at 255 K.

3.2. *The Ehrenfest order of the transition*

An nth order phase transition is defined, following Ehrenfest (1933), as one in which the nth and higher derivatives of G, Gibbs free energy, with respect to T and p show discontinuities. Thus, a first-order transition has discontinuities in V [= $(\partial G/\partial p)_T$] and S [= $(\partial G/\partial T)_p$], and also in H, U *etc.* A second-order transition will have discontinuities in the isobaric thermal expansion coefficient α (= $[(1/V)(\partial V/\partial T)]_p$ = $\{(1/V)[\partial/\partial T(\partial G/\partial p)_T]_p\}$) and the specific heat at constant pressure C_p (= $[T(\partial S/\partial T)_p]$ = $[-T(\partial^2 G/\partial T^2)_p]$; both

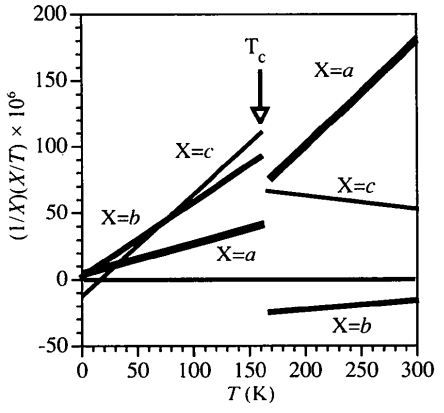

Fig. 3. The values of $[(1/X)(\partial X/\partial T)]$ as functions of temperature. The values were calculated by differentiating the quadratic expressions given in the caption to Fig. 2 (thickest lines $X = a$, medium line $X = b$, thinnest line $X = c$).

Table 2. *Coefficients* ($\times 10^6$ K^{-1}), α_{ij}, *of the thermal expansion tensor below and above the critical temperature*

Temperature interval	α_{11}	α_{22}	α_{33}	α_{13}
70–150 K Ordered phase	18.9	49.3	49.4	−44.0
200–280 K Disordered phase	126.6	−25.7	55.9	−63.8

The principal components, α_i, and the angles between the α_i and the orthonormal crystal axes $\mathbf{d}_{100}$, **b**, **c**

Temperature interval	Eigenvalues ($\times 10^6$ K^{-1})	Eigenvector angles		
70–150 K	−12.4	35.5	90	54.5
	49.3	90	0	90
	80.7	125.5	90	35.5
200–280 K	−25.7	90	0	90
	18.4	59.5	90	30.5
	164.1	149.5	90	59.5

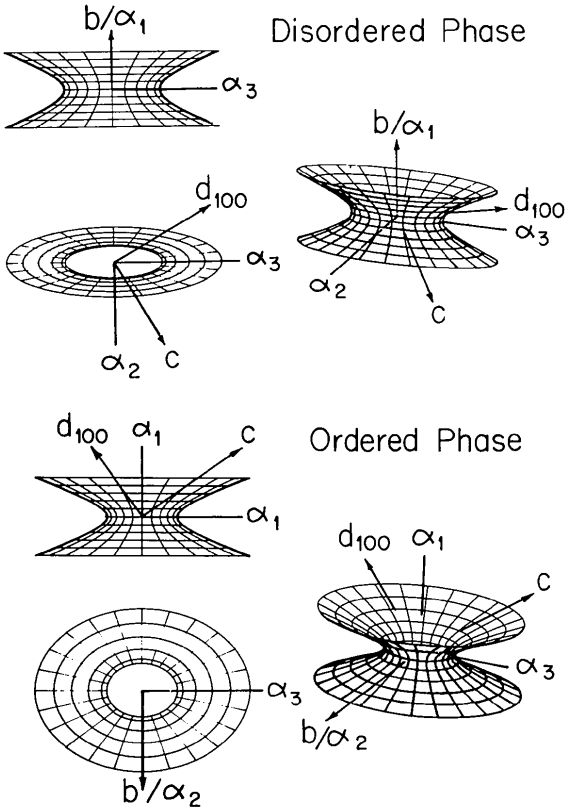

Fig. 4. Diagrams of the representation quadrics (hyperboloids of one sheet) of the thermal expansion tensor for the disordered (combining 280 and 200 K cell dimensions) and ordered phases (combining 150 and 70 K cell dimensions). Three views of each quadric are shown: down two of the principal axes and a bimetric view. The principal axes, α_i, of the quadric are shown and the directions of the orthogonal crystal axes $\mathbf{d}_{100}$, **b** and **c** have been inserted in the diagram. In the disordered phase the imaginary axis of the tensor is along the **b** crystallographic axis and $\mathbf{d}_{100}$ and **c** lie in the α_2, α_3 plane. In the ordered phase the imaginary axis of the tensor lies in the $\mathbf{d}_{100}$,**c** plane, and is normal to **b**, and $\mathbf{d}_{100}$ and **c** lie in the α_1, α_3 plane. Diagrams by Dr A. Banai.

relevant here), and also in the isothermal compressibility and the specific heat at constant volume (not relevant here) (see Berry, Rice & Ross, 1980, p. 864).

The following items of evidence taken together indicate that the transition is of second order as defined by Ehrenfest. The V–T curve (Fig. 5) is continuous but has a change in slope at T_c = 167 K; all three thermal expansion coefficients show discontinuities at 167 K (Fig. 3); there are no superheating or supercooling effects (*i.e.* no hysteresis); the specific heat C_p has a peak but not a discontinuity (Figs. 1 and 6, where ΔC_p in the latter is the excess heat capacity due to the phase transition, obtained by interpolating a smooth curve for the lattice contribution to C_p); superlattice reflections appear below 165 K (Fig. 7). The detailed behaviour of the cell dimensions suggests that the real physical situation is more complicated than that implied by the formal definition.

The C_p–T curve has a peak but not a discontinuity, with the two sets of measurements agreeing reasonably well over most of the anomalous region (Fig. 6), the larger differences occurring in the vicinity of the peak. Superlattice reflections, corresponding to a doubling of the c axis, appear below 165 K. All the superlattice reflections have the same temperature dependence, which is illustrated for three of the stronger reflections in Fig. 7.

3.2.1. *Pressure dependence of critical temperature for ordering.* The results described above allow us to predict the pressure dependence of T_c, using an analogue to the Clapeyron equation developed by Ehrenfest for second-order transitions [see Pippard (1964), equations 8.19 and 9.1]. Ehrenfest's equation can be written as

$$dT_c/dP = T_c[(\partial V/\partial T)_2 - (\partial V/\partial T)_1]/[(C_p)_2 - C_p)_1],$$

where the subscripts 1 and 2 refer to the state of the system just below and just above T_c. A value of $[(\partial V/\partial T)_2 - (\partial V/\partial T)_1]$ is obtained from Fig. 3 and a value of $[(C_p)_2 - (C_p)_1]$ from Fig. 6; using these values

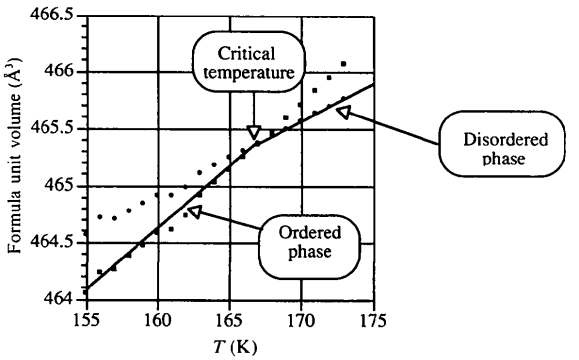

Fig. 5. The variation in volume/formula units of the ordered and disordered phases in the vicinity of T_c (= 167 K), as calculated from the quadratic expressions given in the caption to Fig. 2. As there is no hysteresis, extension of the respective curves above and below T_c is not physically possible but is shown to emphasize the differences in slopes. The values of $(\partial V/\partial T)_P$ per formula unit are 0.108 Å^3 K^{-1} for the ordered phase and 0.057 Å^3 K^{-1} for the disordered phase.

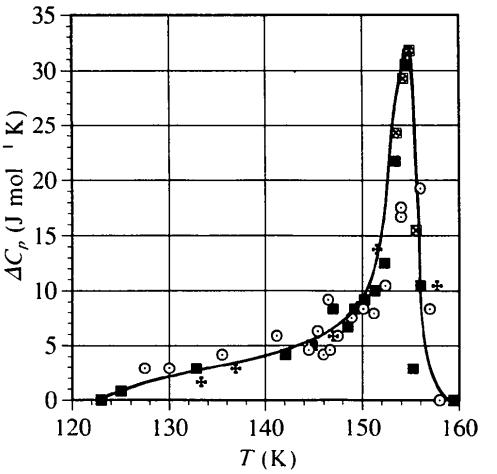

Fig. 6. The excess specific heat in the vicinity of T_c shown in detail; the centred circles are from Dunn, Rahman & Staveley (1978) and the other points from different series of measurements by Boerio-Goates & Westrum (1980). The values of C_{p1}, and C_{p2}, the specific heats just below and above T_c, are 272 and 245 J mol^{-1} K (64.97 and 58.52 cal mol^{-1} K; see Fig. 1 and the discussion in §3.3.1.). The curve is a guide to the eye.

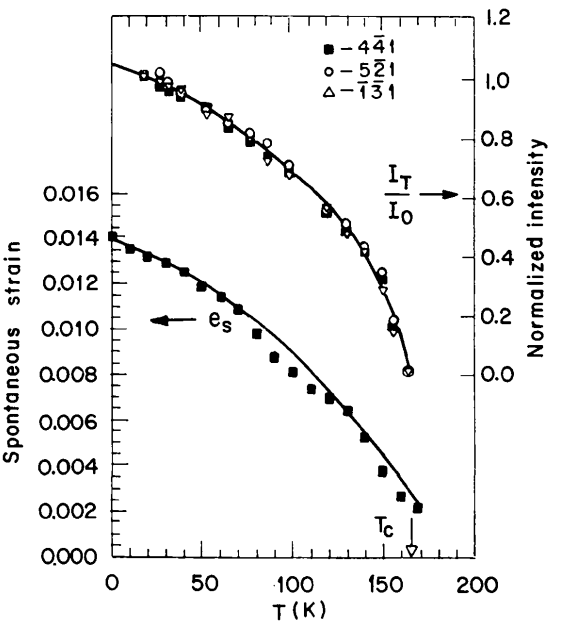

Fig. 7. Upper graph - variation of the normalized intensities (I_T/I_0) of superlattice reflections as a function of temperature (I_0 was estimated for each reflection from a smooth extrapolation of the I–T curve to T = 0 K). Lower graph - the spontaneous strain in the ordered phase of PYRPMA plotted against temperature. The curves shown are guides to the eye.

we calculate that $dT_c/dP \simeq 17$ K kbar^{-1}, if the specific heat values given by Boerio-Goates & Westrum (1980) are used, and about half this amount using those of Dunn, Rahman & Staveley (1978). Thus, application of a pressure of a few kbar should produce the ordered phase of PYRPMA at room temperature. Following Le Chatelier's principle, one would expect the application of pressure to favour ordering.

3.3. *Application of Landau theory*

The Landau theory gives the conditions under which a phase change involving a change of symmetry may be continuous. Details, for all 230 space groups, are given by Stokes & Hatch (1988). The physically irreducible representations for the transition discussed here are Y_1^+ and Y_2^+ and a continuous change is permitted by both Landau and Lifshitz conditions and also under renormalization group analysis. In our description we have maintained analogous cell axes for both phases with consequent differences in the space groups, whereas Stokes & Hatch have followed the converse path. The relationship between the space groups was discussed in HS69.

The long-range order parameter $Q = |1-2p|$, where p is the probability of finding a pyrene molecule in the unfavoured orientation; in a continuous transition, as in PYRPMA, Q is unity at absolute zero and decreases smoothly (for a 1:1 composition) to zero at the critical temperature. Modern theoretical treatments of order-disorder phase transitions are often given in terms of critical exponents (Berry, Rice & Ross, 1980, p. 873; Lifshitz & Pitaevskii, 1980; Stanley, 1971; Tolédano & Tolédano, 1987), where (to a first approximation)

$$f(1 - T/T_c) = A(1 - T/T_c)^{\lambda}.$$

Here $f(1 - T/T_c)$ is a physically measurable quantity, such as, in the present context, ΔC_p, spontaneous strain or the intensity of a superlattice reflection. The value of the critical exponent, λ, depends on the physical property under investigation and the nature of the transition which can, in turn, be inferred from the values of the critical exponents, measured as close as possible to the critical temperature. For example, C_p for the upper phase change in 3(thiourea).CCl_4 was fitted to an equation of the type above with a critical exponent of -0.31, using measured values within 1° of the critical temperature of 67.166 K (Seki, Matsuo & Suga, 1990).

As our measurements cover a wide temperature range but are sparse close to T_c, we preferred to follow the method of analysis proposed by Salje (1990, see p.14), which involves a rather drastic extension of classical Landau theory (see Lifshitz & Pitaevskii, 1980, Ch. XIV) to large values of the order parameter. Following Salje (1990), PYRPMA is a co-elastic crystal [non-ferroic in the nomenclature used by Stokes & Hatch (1988)] where 'elastic and strain anomalies...are correlated with the structural phase transition'. The spontaneous strain in the ordered phase, given in terms of the Vogt coefficients e_j, can be calculated (Salje, 1990, p. 26-27), as a function of temperature, from the measured cell dimensions of the ordered phase (not subscripted) and the extrapolated cell dimensions of the disordered phase (subscripted) using

$$e_1 = a/a_0 - 1,\ e_2 = b/b_0 - 1,\ e_3 = (c\sin\beta^*/c_0\sin\beta_0^*) - 1,$$
$$e_5 = (a\cos\beta^*/a_0\sin\beta_0^*) - (c\cos\beta^*/c_0\sin\beta_0^*).$$

The (scalar) spontaneous strain in the ordered phase is then defined as $e_s = (\Sigma e_j^2)^{1/2}$ and is proportional to the square of the order parameter Q. The spontaneous strain is plotted against temperature in Fig. 7 and has a shape somewhat similar to that of the superlattice intensity-temperature curve also shown in Fig. 7 (the superlattice intensity is also proportional to Q^2). If the phase transition is tricritical (the intermediate stage between continuous and discontinuous transitions), then it follows from Landau theory that the fourth power of the order parameter is linearly proportional to T; this is indeed found in the plot of $(e_s)^2$ against T (Fig. 8). A further test of the tricritical nature of the transition can be made using the intensities of the superlattice reflections shown in Fig. 7. The squares of the normalized intensities are plotted against T in Fig. 8. Although the plot is linear, it extrapolates to $Q^4 = 1.14$ [$Q(T\rightarrow 0) = 1.03$], indicating that the intensities measured at the lower temperatures are systematically larger than those predicted by Q^4 temperature dependence. We do not have an explanation.

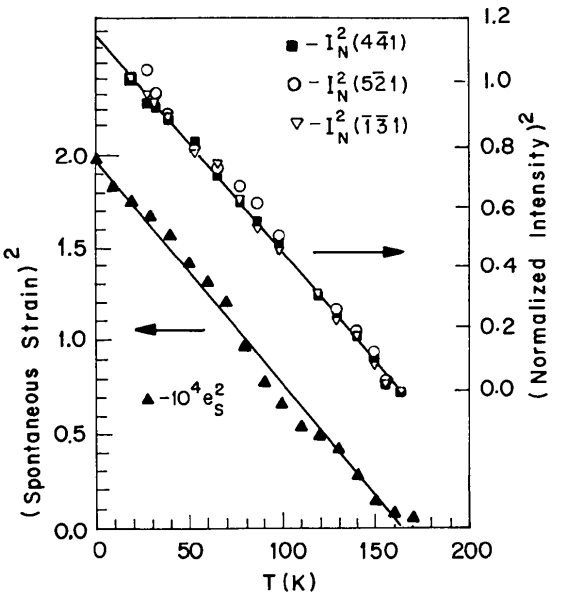

Fig. 8. Upper graph - the square of the normalized intensity plotted against temperature for three superlattice reflections of the ordered phase of PYRPMA. Lower graph - the square of the spontaneous strain in the ordered phase of PYRPMA plotted against temperature.

Finally, we test whether the dependence of the excess specific heat on temperature (Fig. 6) is compatible with a tricritical transition by plotting $\log(\Delta C_p)$ against $\log(T_c - T)$, where T_c = 155 K (Fig. 9). The log-log plot shows that ΔC_p, as a function of $(1 - T/T_c)$, is not well represented by the power law equation $\Delta C_p = A[1 - (T/T_c)]^{-\alpha}$. A forced linear fit gives α = 0.77, whereas α = 0.5 for a tricritical transition (Salje, 1990, p. 120).

In summary, the theory of an almost tricritical phase transition with a simple one-component order parameter indicates that the power-law exponents β, obtained from the spontaneous strain or from the temperature dependence of the intensities of the superlattice reflections, should be 0.25 and α, obtained from ΔC_p, should be 0.5 (Salje, 1990). We find good agreement with experiment for the first of these predictions but not for the second. There is a physical difference in that the diffraction measurements cover the whole temperature range below T_c, while ΔC_p is restricted to between T_c - 35 and T_c.

3.4. *Comparison with other systems*

From a formal, crystallographic point of view, the ordering of the sublattice of pyrene molecules in PYRPMA is entirely equivalent to the much studied disorder-order transition in chloranil with $T_c \simeq 92$ K [NQR: Richardson (1963); Chihara & Nakamura (1973); C_p: Chihara & Masukane (1973); X-ray diffraction: Terauchi, Sakai & Chihara (1975); neutron diffraction: Ellenson & Kjems (1977); Baudour, Delugeard, Cailleau, Sanqueur & Zeyen (1981); Baudour & Meinnel (1982)]. Chloranil crystallizes in space group $P2_1/a$ (Z = 2) above T_c [crystal structure determined in detail at 295 K (Chu, Jeffrey & Sakurai, 1962) and 110 K (van Weperen & Visser, 1972)] and transforms (single crystal-to-single crystal, with the retention of axial directions) below T_c to space group $P2_1/n$, with doubling of the c axis, just as in PYRPMA; an outline of the structure at 77 K was determined using eight superlattice intensities (Terauchi, Sakai & Chihara, 1975). The C_p measurements give ΔH_{tr} = 38 J mol^{-1}, ΔS_{tr} = 0.41 J mol^{-1} K. Below T_c, the two chloranils at independent symmetry centres are mutually tilted by a few degrees. Integrated intensities between 95 and 4 K were measured by X-ray diffraction for the $(\bar{1}0,13)$ superlattice reflection (Terauchi, Sakai & Chihara, 1975) and by neutron diffraction for $(\bar{1}07)$ (Ellenson & Kjems, 1977) (indices refer to the $P2_1/n$ cell). A theoretical treatment developed by Chihara, Nakamura & Tachiki (1973) gave excellent agreement with both X-ray diffraction and NQR measurements.

From a chemical and structural point of view, the disorder-to-order phase transition in PYRPMA is similar to those in the π-molecular compounds naphthalene···TCNB and anthracene···TCNB [see Lefebvre, Odou, Muller, Mierzejewski & Luty (1989), who give references to earlier work; TCNB = 1,2,4,5-tetracyanobenzene], which are isostructural but not isomorphous. Ordering occurs at ~76 and ~210 K, respectively; the space group changes from $C2/m$ to $P2_1/a$. The aromatic molecules take up one orientation above T_c and two below; the TCNBs do not change. In both groups, it is the $D\cdots A$ interactions between different stacks which dominate (see Fig. 4 of Lefebvre *et al.* and Fig. 8 of HMS94).

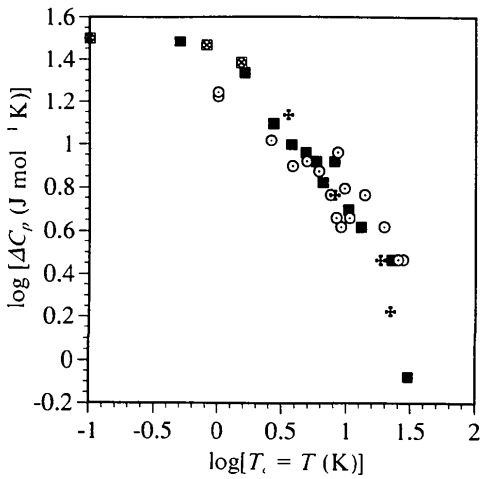

Fig. 9. Log-log plot of the excess heat capacity (ΔC_p) against deviation from critical temperature in the vicinity of the phase transition; the values of ΔC_p were taken from Fig. 6 - the centred circles are from Dunn, Rahman & Staveley (1978; T_c = 156 K) and the other points from different series of measurements by Boerio-Goates & Westrum (1980; T_c = 155 K).

4. Thermodynamic parameters for PYRPMA

As C_p values have been reported for pyrene (Wong & Westrum, 1971), PMDA (Dunn, Rahman & Staveley, 1978) and PYRPMA (Dunn, Rahman & Staveley, 1978; Boerio-Goates & Westrum, 1980) for the range 0-300 K, it is possible to derive (within certain limitations) values for the enthalpy and entropy of formation of PYRPMA over this temperature range. Our discussion here refers exclusively to molar quantities of the crystalline phases of pyrene, PMDA and PYRPMA. The enthalpy functions of the crystalline phases are calculated as follows from the calorimetric data,

$$H_T - H(0) = \int_0^T C_p \mathrm{d}T,$$

the values of the integration constants $H(0)$ being unknown. The values of $H_T - H(0)$ for the three phases were taken from the above sources; the function $H_T - H(0)$ is smooth in the region 0-300 K for PMDA, which has no phase transformations in this range, and virtually so for pyrene and PYRPMA, despite their phase transformations which have negligible effect on the integrals. In the discussion that follows, we assume

that the molecular compound is stable with respect to dissociation into its components over the temperature range 0-300 K.

The enthalpy of formation of PYRPMA from its component molecules at temperature T is

$$[\Delta H_f(\mathrm{P/PM})]_T = [H_T]_{(\mathrm{P/PM})} - \{[H_T]_\mathrm{P} + [H_T]_\mathrm{PM}\}, \quad (1)$$

where P and PM are abbreviations for pyrene and PMDA, respectively. In the temperature range 160-300 K, P/PM = disordered PYRPMA and P = α-pyrene, while P/PM = ordered PYRPMA and P = β-pyrene for the temperature range 0-100 K. The function is ill-defined in the range 100-160 K because of the phase transformations in pyrene and PYRPMA. It is convenient to group the integration constants together as $\Sigma H(0) = \{H(0)_{\mathrm{P/PM}} - [H(0)_\mathrm{P} + H(0)_\mathrm{PM}]\}$, where, in principle, different values of $H(0)$ should be used for the different phases of pyrene and PYRPMA. The difference of the enthalpy functions, which is given by

$$\delta[\Delta H_f(\mathrm{P/PM})]_T = [H_T - H(0)]_{(\mathrm{P/PM})} - \{[H_T - H(0)]_\mathrm{P} + [H_T - H(0)]_\mathrm{PM}\}, \quad (2)$$

can be determined from the measured calorimetric values. This function, which is plotted in Fig. 10, is the change in $[\Delta H_f(\mathrm{P/PM})]$ on heating from 0 to TK. If values of $\Sigma H(0)$ were known, then one could obtain the absolute values of $[\Delta H_f(\mathrm{P/PM})]$ as a function of temperature. As Dr Staveley has pointed out to us, one could obtain $[\Delta H_f(\mathrm{P/PM})]$ at 300 K (say) from measurements of the enthalpies of solution of P, PM and P/PM (extrapolated to infinite dilution). Such an experiment has been carried out for quinhydrone and its components (Suzuki & Seki, 1953; Artiga, Gaultier, Haget & Chanh, 1978), but not for our present system.

The entropies are calculated as follows

$$S_T - S(0) = \int_0^T C_p \, \mathrm{d}\ln T. \quad (3)$$

If the third law of thermodynamics applies, then $S(0) = 0$. An expression analogous to (2), but with $\Sigma S(0) = 0$ because of the third law of thermodynamics, can be written for the entropy of formation of PYRPMA from its component molecules at temperature T (Fig. 11). The molecular compound is entropy-stabilized except within the range 0-30 K; it must be enthalpy-stabilized within the range 0-30 K but we are not able to say whether there is an enthalpy contribution to the stabilization {*i.e.* $[\Delta H_f(\mathrm{P/PM})]_T$ negative} outside this range.

We can set limits on the value of $\Sigma H(0)$ in the following way. The free energy of formation of PYRPMA is

$$[\Delta G_f(\mathrm{P/PM})]_T = [\Delta H_f(\mathrm{P/PM})]_T - T[\Delta S_f(\mathrm{P/PM})]_T = \{\textstyle\sum H(0) + \delta[\Delta H_f(\mathrm{P/PM})]_T\} - T[\Delta S_f(\mathrm{P/PM})]_T.$$

We plot $\delta[\Delta H_f(\mathrm{P/PM})]_T - T[\Delta S_f(\mathrm{P/PM})]_T$, which we call the net free energy (of PYRPMA), against T in Fig. 12. From our assumption that PYRPMA is stable between 0 and 300 K it follows that $[\Delta G_f(\mathrm{P/PM})]_T$ is negative over this range and thus that $\Sigma H(0)$ must be less than 5 J mol^{-1}.

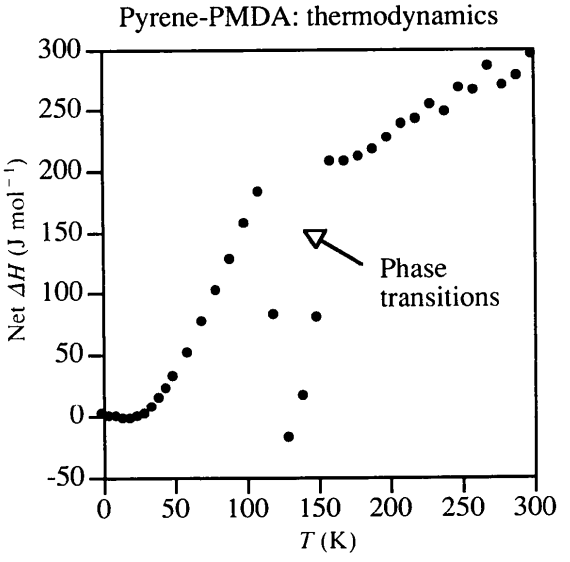

Fig. 10. The difference between the enthalpy functions, $\delta[\Delta H_f(\mathrm{P/PM})]_T$, for PYRPMA (see text for definition) as a function of temperature. The values are not well defined in the range 100-160 K because of the phase transformation in pyrene and the order-disorder transition in PYRPMA.

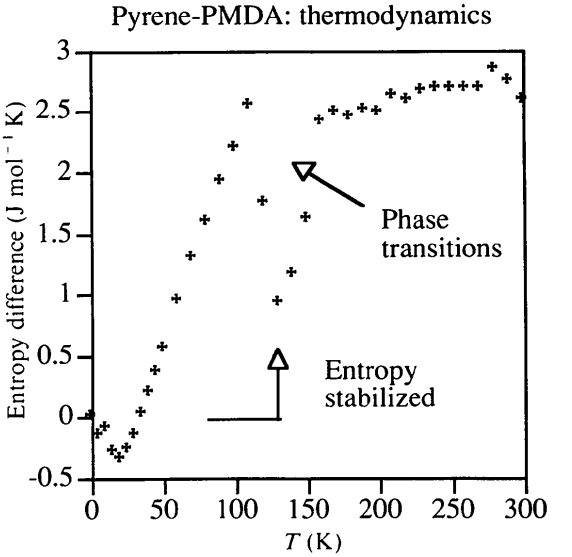

Fig. 11. The entropy of formation of PYRPMA, as a function of temperature. The values are not well defined in the range 100-160 K because of the phase transformation in pyrene and the order-disorder transition in PYRPMA.

The value of $[\Delta S_f(\text{P/PM})]_T$ at 300 K is 2.7 J mol^{-1} K. The difference in configurational entropy between fully ordered and fully disordered PYRPMA phases should be approximately $R\ln 2$ = 5.76 J mol^{-1} K. The measured entropy of formation contains contributions from configurational and thermal-vibration entropy (other contributions are neglected) and comparison of these two values implies that the thermal-vibration entropy of PYRPMA is about 3 J mol^{-1} K less than the sum of the thermal-vibration entropies of pyrene and PMDA. Excess specific heat due to the order-disorder transition appears only above 120 K, where the long-range order parameter is about 0.75 (see Fig. 7) - thus, the entropy of the transition as found from the excess specific heat would be expected to be about 4.3 J mol^{-1} K, whereas the measured value is 1.34 J mol^{-1} K. Perhaps differences in the thermal-vibration entropies (of ordered and disordered PYRPMA phases) could account for this discrepancy.

5. Concluding remarks

The order-disorder transition at ~160 K has been shown, from the measurement of the cell dimensions and superlattice intensities as functions of temperature, to be second order in terms of Ehrenfest's classification; this agrees with conclusions drawn from earlier calorimetric measurements. Ordering is due to small changes in the mutual orientations of the pyrenes, while the PMDAs are closely packed over the whole temperature range. There are indications that the non-bonded interactions between >C—H groups of pyrene and O atoms of PMDA are dominant in the ordering process (see HMS94) rather than >C—H···H—C< interactions, as inferred by Allen, Boeyens & Levendis (1989). In formal terms, the structural changes on ordering in PYRPMA are very similar to those which occur in the ordering of chloranil. In chemical terms, there is rather more resemblance to the transitions in the π-molecular compounds naphthalene···TCNB and anthracene···TCNB. We consider that intermolecular (packing) interactions, rather than electronic or charge-transfer interactions, are responsible for all these transitions. Power-law fits of the temperature dependence of the spontaneous strain and the superlattice intensities suggest that the transition of the co-elastic crystals is tricritical in terms of extended Landau theory; however, the excess (due to the transition) specific heats do not fit this suggestion very well.

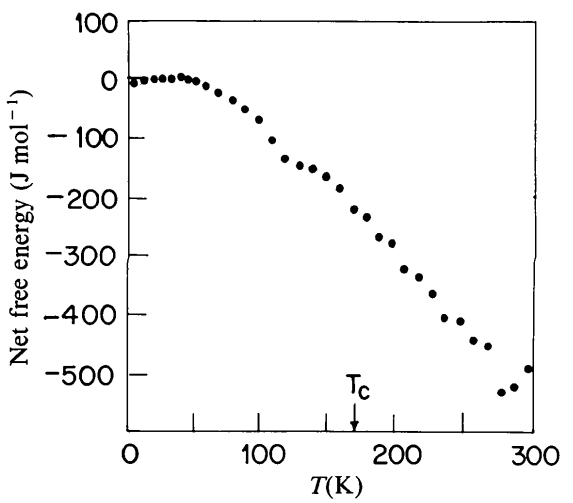

Fig. 12. Plot of 'net free energy' $\{\delta[\Delta H_f(\text{P/PM})]_T - T[\Delta S_f(\text{P/PM})]_T\}$ against T.

With regard to the study of the phase transition, X-ray diffraction methods provide two lines of approach - measurement of cell dimensions and superlattice intensities, as functions of temperature. Experience shows that cell dimensions measured by current standard diffractometric techniques using Mo $K\alpha$ have limited precision (e.s.d.'s of ~0.01-0.02 Å; *cf.* Taylor & Kennard, 1986); measurements at high Bragg angles, using Cu $K\alpha$, appear to be essential when more accurate cell dimensions are required. More effort could have been spent in measuring superlattice intensities as close to T_c as possible in order to determine the 'critical exponent' of modern phase-transition theory, while determination of crystal structures at a number of intermediate temperatures (as carried out but not reported here) appears to have been largely redundant. Attempts should have been made, despite the problems involved in doing this by diffractometry, to determine whether the long-range order superlattice Bragg reflections below T_c are replaced by short-range order diffuse scattering above T_c.

This work has been supported by the Fund of the Vice President for Research and the Fund for Promotion of Research at Technion, by the CSIR (Pretoria) and by a number of NIH grants. We are grateful to Drs Jessen & Küppers (Kiel) for a copy of their thermal expansion program, Dr Abraham Banai (Mathematics, Technion) for writing the *BASIC* program used for obtaining Fig. 4 and Dr L. A. K. Staveley (Oxford) and Professor E. F. Westrum Jr (Ann Abor) for useful comments on the thermodynamics. The referees have also been very helpful.

References

ALLEN, C. C., BOEYENS, J. C. A. & LEVENDIS, D. C. (1989). *S. Afr. J. Chem.* **42**, 38-42.

ARTIGA, A., GAULTIER, J., HAGET, Y. & CHANH, N. B. (1978). *J. Chim. Phys.* **75**, 379-383.

BAUDOUR, J. L., DELUGEARD, Y., CAILLEAU, H., SANQUEUR, M. & ZEYEN, C. M. E. (1981). *Acta Cryst.* B**37**, 1553-1557.

BAUDOUR, J. L. & MEINNEL, J. (1982). *Acta Cryst.* B**38**, 472-479.

BERRY, R. S., RICE, S. A. & ROSS, J. (1980). *Physical Chemistry*. New York: John Wiley.

BOERIO-GOATES, J. & WESTRUM, E. F. JR (1980). *Mol. Cryst. Liq. Cryst.* **60**, 249-266.

CHIHARA, H. & MASUKANE, K. (1973). *J. Chem. Phys.* **59**, 5397-5403.

CHIHARA, H. & NAKAMURA, N. (1973). *J. Chem. Phys.* **59**, 5392-5396.

CHIHARA, H., NAKAMURA, N. & TACHIKI, M. (1973). *J. Chem. Phys.* **59**, 5387-5391.
CHU, S. S. C., JEFFREY, G. A. & SAKURAI, T. (1962). *Acta Cryst.* **15**, 661-671.
DUNN, A. G., RAHMAN, A. & STAVELEY, L. A. K. (1978). *J. Chem. Thermodyn.* **10**, 787-796.
EHRENFEST, P. (1933). *Proc. Acad. Sci. Amsterdam*, **36**, 153-157.
ELLENSON, W. D. & KJEMS, J. K. (1977). *J. Chem. Phys.* **67**, 3619-3623.
HERBSTEIN, F. H. (1971). In *Perspectives in Structural Chemistry*, edited by J. D. DUNITZ & J. A. IBERS, Vol. IV, pp.166-395. London and New York: John Wiley.
HERBSTEIN, F. H., MARSH, R. E. & SAMSON, S. (1994). *Acta Cryst.* B**50**, 174-181.
HERBSTEIN, F. H. & SNYMAN, J. A. (1969). *Philos. Trans. R. Soc. London Ser. A*, **264**, 635-666.
JESSEN, S. M. & KÜPPERS, H. (1990). *Z. Krist. Collected Abstracts of XIIth European Crystallographic Meeting, Moscow*, Vol. I, p. 349 (published as Supplement No. 2 of 1990).
JESSEN, S. M. & KÜPPERS, H. (1991). *J. Appl. Cryst.* **24**, 239-241.
LEFEBVRE, J., ODOU, G., MULLER, M., MIERZEJEWSKI, A. & LUTY, T. (1989). *Acta Cryst.* B**45**, 323-336.
LIFSHITZ, E. M. & PITAEVSKII, L. P. (1980). In *Course of Theoretical Physics*, 3rd ed., *Statistical Physics*, Part 1, Vol. 5, ch. 10, edited by L. D. LANDAU, & E. M. LIFSHITZ. Oxford: Pergamon Press.
NYE, J. F. (1967). *Physical Properties of Crystals*, 1st ed. Oxford: Clarendon Press.
PARSONAGE, N. G. & STAVELEY, L. A. K. (1978). *Disorder of Crystals*. New York: Oxford Univ. Press.
PIPPARD, A. B. (1964). *The Elements of Classical Thermodynamics*. Cambridge: Cambridge Univ. Press.
RICHARDSON, C. B. (1963). *J. Chem. Phys.* **38**, 510-515.
SALJE, E. K. H. (1990). *Phase Transitions in Ferroelastic and Coelastic Crystals, Cambridge Topics in Mineral Physics and Chemistry*. Cambridge: Cambridge Univ. Press.
SAMSON, S., GOLDISH, E. & DICK, C. J. (1980). *J. Appl. Cryst.* **13**, 425-432.
SEKI, M., MATSUO, T. & SUGA, H. (1990). *J. Incl. Phenom. Mol. Recogn. Chem.* **9**, 243-251.
STANLEY, H. E. (1971). *Introduction to Phase Transitions and Critical Phenomena*. Oxford: Oxford Univ. Press.
STOKES, H. T. & HATCH, D. M. (1988). *Isotropy Subgroups of the* 230 *Crystallographic Space Groups*. Singapore: World Scientific.
SUZUKI, K. & SEKI, S. (1953). *Bull. Chem. Soc. Jpn*, **26**, 372-380.
SVENSSON, C. & ABRAHAMS, S. C. (1986). *Acta Cryst.* B**42**, 280-286.
TAYLOR, R. & KENNARD, O. (1986). *Acta Cryst.* B**42**, 112-120.
TERAUCHI, H., SAKAI, T. & CHIHARA, H. (1975). *J. Chem. Phys.* **62**, 3832-3833.
TOLÉDANO, J.-C. & TOLÉDANO, P. (1987). *The Landau Theory of Phase Transitions*. Singapore: World Scientific.
WEPEREN, K. J. VAN & VISSER, G. J. (1972). *Acta Cryst.* B**28**, 338-342.
WONG, W.-K. & WESTRUM, E. F. JR (1971). *J. Chem. Thermodyn.* **3**, 105-124.

Acta Cryst. (1994). B**50**, 191–200

Pyridinium Picrate - the Structures of Phases I and II. Correction of Previous Report for Phase I. Study of the Phase Transformation

BY MARK BOTOSHANSKY, FRANK H. HERBSTEIN AND MOSHE KAPON

Department of Chemistry, Technion-Israel Institute of Technology, Haifa 32000, *Israel*

(*Received* 5 *February* 1993; *accepted* 11 *August* 1993)

Abstract

Pyridinium picrate, $C_5H_6N^+.C_6H_2N_3O_7$, was reported [Kofler (1944). *Z. Elektrochem.* **50**, 200-207] to exist in two crystalline phases, one (I) being stable below 343 K and the other (II) between 343 K and the melting point (~438 K). The room-temperature structure of phase I, studied by two-dimensional methods, has been reported [Talukdar & Chaudhuri (1976). *Acta Cryst.* B**32**, 803-808]. We were led to reinvestigate the system by a number of unusual features in Kofler's description of the phase behaviour. Single crystals of phase I were grown from solution and those of phase II from the melt. We have determined the structure of both phases, including analysis of the thermal motion of the picrate ions, which was found to be appreciably larger in phase II than in phase I. The reported structure of phase I was found to be incorrect, although there were no warning signs; the error was caused by confusion between a centre and twofold screw axis in projection down [010]. The packing units in the two phases are nearly identical and consist of hydrogen-bonded cation-anion pairs. These are packed in stacks, with the ion-pairs superimposed in parallel array in phase I whereas those in phase II are antiparallel; the transition between the two phases, therefore, cannot be expected to be single crystal to single crystal, as indeed it is not. Differential scanning calorimetry (DSC) and variable-temperature powder X-ray diffraction photography show that the transition occurs at 383 K. Kofler appears to have been misled by a colour change in the phase I crystals at 343 K, which we have also observed but cannot explain. The DSC measurements give ΔH_{trans} = 6.8 kJ mol^{-1} and ΔH_{fus} = 31.2 kJ mol^{-1}. The transition has proved not to be reversible under our experimental conditions; for example, phase II crystals remain unchanged after 24 h at 353 K. This suggests that the temperature at which the crystalline phases